ORIGINAL ARTICLE

# CD148 Deficiency in Fibroblasts Promotes the Development of Pulmonary Fibrosis

Konstantin Tsoyi[1], Xiaoliang Liang[1], Giulia De Rossi[2], Stefan W. Ryter[3], Kevin Xiong[4], Sarah G. Chu[4], Xiaoli Liu[4], Bonna Ith[4], Lindsay J. Celada[1], Freddy Romero[1], Matthew J. Robertson[1], Anthony J. Esposito[4], Sergio Poli[4], Souheil El-Chemaly[4], Mark A. Perrella[4], YuanYuan Shi[5], James Whiteford[2], and Ivan O. Rosas[1,4]

[1]Section of Pulmonary, Critical Care and Sleep Medicine, Department of Medicine, Baylor College of Medicine, Houston, Texas; [2]William Harvey Research Institute, Barts and the London School of Medicine and Dentistry, Queen Mary University of London, London, United Kingdom; [3]Division of Pulmonary and Critical Care Medicine, Department of Medicine, Weill Cornell Medicine, New York, New York; [4]Division of Pulmonary and Critical Care Medicine, Department of Medicine, Brigham and Women's Hospital, Harvard Medical School, Boston, Massachusetts; and [5]School of Life Sciences, Beijing University of Chinese Medicine, Beijing, China

## Abstract

**Rationale:** CD148/PTRJ (receptor-like protein tyrosine phosphatase η) exerts antifibrotic effects in experimental pulmonary fibrosis via interactions with its ligand syndecan-2; however, the role of CD148 in human pulmonary fibrosis remains incompletely characterized.

**Objectives:** We investigated the role of CD148 in the profibrotic phenotype of fibroblasts in idiopathic pulmonary fibrosis (IPF).

**Methods:** Conditional CD148 fibroblast-specific knockout mice were generated and exposed to bleomycin and then assessed for pulmonary fibrosis. Lung fibroblasts (mouse lung and human IPF lung), and precision-cut lung slices from human patients with IPF were isolated and subjected to experimental treatments. A CD148-activating 18-aa mimetic peptide (SDC2-pep) derived from syndecan-2 was evaluated for its therapeutic potential.

**Measurements and Main Results:** CD148 expression was downregulated in IPF lungs and fibroblasts. In human IPF lung fibroblasts, silencing of CD148 increased extracellular matrix production and resistance to apoptosis, whereas overexpression of CD148 reversed the profibrotic phenotype. CD148 fibroblast-specific knockout mice displayed increased pulmonary fibrosis after bleomycin challenge compared with control mice. CD148-deficient fibroblasts exhibited hyperactivated PI3K/Akt/mTOR signaling, reduced autophagy, and increased p62 accumulation, which induced NF-κB activation and profibrotic gene expression. SDC2-pep reduced pulmonary fibrosis *in vivo* and inhibited IPF-derived fibroblast activation. In precision-cut lung slices from patients with IPF and control patients, SDC2-pep attenuated profibrotic gene expression in IPF and normal lungs stimulated with profibrotic stimuli.

**Conclusions:** Lung fibroblast CD148 activation reduces p62 accumulation, which exerts antifibrotic effects by inhibiting NF-κB–mediated profibrotic gene expression. Targeting the CD148 phosphatase with activating ligands such as SDC2-pep may represent a potential therapeutic strategy in IPF.

**Keywords:** CD148; fibroblast; idiopathic pulmonary fibrosis; nuclear factor-kappa-B; syndecan-2

Idiopathic pulmonary fibrosis (IPF) is a chronic, progressive lung disease characterized by lung scarring (1). The incidence of IPF is age dependent, and IPF has a high rate of mortality, with a median survival of 3 years (1). The pathogenesis of IPF involves dysregulated wound healing with continuous damage to lung epithelium, fibroblast/myofibroblast activation, and excessive

(Received in original form August 6, 2020; accepted in final form March 30, 2021)

Supported by NHLBI grant P01 HL114501 (I.O.R.) and by NHLBI grant T32 5T32HL007633-32 and National Institute of Arthritis and Musculoskeletal and Skin Diseases grant K01 5K01AR074558 (K.T.).

Author Contributions: K.T., S.G.C., J.W., and I.O.R. designed the study. K.T., X. Liang, G.D.R., S.W.R., K.X., S.G.C., X. Liu, B.I., S.P., and I.O.R. performed the experiments, contributed materials and analyzed data. L.J.C., F.R., M.J.R., A.J.E., S.E.-C., Y.Y.S., and M.A.P. contributed intellectual input. K.T., S.W.R., S.G.C., and I.O.R. wrote the manuscript.

Correspondence and requests for reprints should be addressed to Ivan O. Rosas, M.D., Section of Pulmonary, Critical Care and Sleep Medicine, Department of Medicine, Baylor College of Medicine, 7200 Cambridge Street, Houston, TX 77030. E-mail: ivan.rosas@bcm.edu.

This article has a related editorial.

This article has an online supplement, which is accessible from this issue's table of contents at www.atsjournals.org.

Am J Respir Crit Care Med Vol 204, Iss 3, pp 312–325, Aug 1, 2021

Originally Published in Press as DOI: 10.1164/rccm.202008-3100OC on March 30, 2021
Internet address: www.atsjournals.org

## At a Glance Commentary

**Scientific Knowledge on the Subject:** Idiopathic pulmonary fibrosis (IPF) is a pulmonary disease involving fibrotic changes of the lung with unknown etiology, for which there is no cure. The pathogenesis of IPF involves dysregulated wound healing, damage to lung epithelium, fibroblast/myofibroblast activation, and excessive extracellular matrix production, leading to aberrant lung remodeling. The receptor-like protein tyrosine phosphatase $\eta$ (CD148) exerts antifibrotic effects in experimental pulmonary fibrosis via interactions with its ligand syndecan-2; however, the role of CD148 in fibroblast activation remains unknown.

**What This Study Adds to the Field:** In this study, we demonstrate that CD148 expressed in lung fibroblasts can confer antifibrotic effects in human and experimental pulmonary fibrosis. CD148-deficient fibroblasts exhibited hyperactivated PI3K/Akt/mTOR signaling, reduced autophagy, and increased p62 accumulation, leading to NF-$\kappa$B activation, which we identify as a novel mechanism regulating profibrotic gene expression. CD148-targeting peptides can exert antifibrotic effects and show therapeutic potential in experimental and human fibrosis.

extracellular matrix (ECM) production, leading to aberrant lung remodeling (2). Because activated fibroblasts and myofibroblasts are among the key effectors of organ fibrogenesis, determining the molecular mechanisms underlying their profibrotic phenotype may accelerate therapeutic development in IPF (2). Although existing antifibrotic therapies can slow the progression of the disease (3, 4), none can reverse existing fibrosis. Thus, there remains an urgent unmet need to identify new therapeutic targets in IPF.

PTPRJ/CD148 (receptor-like protein tyrosine phosphatase-$\eta$) is expressed throughout the hematopoietic system and in the lung, pancreas, thyroid, kidney, mammary glands, and nervous system. CD148 consists of 1,337 amino acids with a single phosphatase domain containing the conserved motif (I/V)HCXAGXGR(S/T)G common to protein tyrosine phosphatases (PTPs) (5). CD148 can regulate cell proliferation, apoptosis, migration, and invasion in multiple cancers (6–8). CD148 can dephosphorylate and inactivate proteins that regulate mitogenic signals (e.g., PDGF, EGF, and VEGF) and act as a putative negative regulator of growth factor receptor signaling via PTP activity (9, 10). Moreover, CD148 can negatively regulate PI3K/Akt signaling by dephosphorylating p85 (the regulatory subunit of PI3K) (11, 12). Hyperactivation of PI3K signaling and shared phenotypes between profibrotic fibroblasts derived from IPF lung and cancer cells (e.g., increased invasiveness, migration, and resistance to cell death) suggest a contributory role of CD148 in IPF (13–15). Here, we sought to delineate the mechanism(s) by which CD148 regulates fibroblast activation and its role as a therapeutic target in IPF.

Syndecans are cell surface heparan sulfate proteoglycans that regulate many cellular functions including proliferation, migration, and cell survival (16). We have shown that syndecan-2 (SDC2), a ligand of CD148, is highly expressed in IPF lungs and alveolar macrophages (17). Transgenic overexpression of SDC2 or treatment with SDC2 attenuated experimental lung fibrosis via CD148 (18), which is consistent with experimental reports in endothelial and T cells (19–20). However, the precise role of fibroblast CD148 in the pathogenesis of human pulmonary fibrosis is largely unexplored. Some of the results of these studies have been previously reported in the form of an abstract (21).

## Methods

### Primary Pulmonary Fibroblasts

The institutional review board at Brigham and Women's Hospital approved all experiments. Lung fibroblasts were isolated from lung transplantation recipients with IPF or nonfibrotic lungs. Mouse lung fibroblasts were isolated as described (22). Fibroblasts were cultured in Dulbecco's modified Eagle medium containing 10% FBS and antibiotics (Corning) in humidified incubators at 37°C and 10% $CO_2$. To induce Cre recombinase expression in *Ptprj*$^{fl/fl}$/Col1a2-Cre-ER(T)$^{+/0}$ or Col1a2-Cre-ER(T)$^{+/0}$ lung fibroblasts, cells were treated with 4-hydroxytamoxifen (1 $\mu$M).

### Mice

All protocols were approved by the Brigham and Women's Hospital Standing Committee for Animal Welfare. C57BL/6 mice (Charles River) were used at 8 weeks of age. GFP-LC3 (light chain-3B) transgenic mice were described (23). To generate fibroblast-specific CD148-knockout mice, transgenic Col1a2$^{Cre-ER(T)+/0}$ and *Ptprj*$^{fl/fl}$ mice, which possess loxP sites on both sides of exon 18, a transmembrane domain of *Ptprj* (Jackson Laboratory), were crossbred. *Ptprj*$^{fl/fl}$ Col1a2$^{Cre-ER(T)+/0}$ mice (8–10 wk old) or control Col1a2$^{Cre-ER(T)+/0}$ mice were administered tamoxifen (75 mg/kg i.p.) for 5 days before experimental treatments and every 72 hours until death (*see* Figure E11 in the online supplement).

### Bleomycin Model of Pulmonary Fibrosis

Lung fibrosis was elicited in mice by bleomycin (BLM) (0.75 mg/kg, intratracheal) (Cayman Chemical); control mice received an equal volume of saline. Mice were killed 21 days after BLM instillation. BAL fluids were analyzed for immune cell counts. The left lung was analyzed for hydroxyproline (18). The right lung lobes were assessed for gene expression and histology.

### SDC2-ED 18-aa Peptide Administration

SDC2-ED 18-aa peptide (SDC2-pep; 0.5 mg/kg in 50 $\mu$l PBS) or PBS (vehicle) was administered at Days 10, 12, 14, 16, and 18 after BLM or saline treatment in mouse strains by intranasal instillation. Mice were killed at Day 24.

### Precision-Cut Lung Slices

Precision-cut lung slices (PCLS) from control and IPF lungs were prepared as described (24, 25), and transfected with Scr, shCD148, empty vector, or pLenti-GIII-CD148-HA lentiviral particles (1–1.5 multiplicity of infection per slice). Twelve hours later, PCLS were incubated $\pm$ SDC2-pep (5 $\mu$M) for 72 hours. PCLS were subjected to immunofluorescent staining or gene expression analysis.

### Histopathology and Immunofluorescent Costaining

Human lung sections were fixed and immunostained for $\alpha$-SMA and CD148. Mouse lungs were collected on Day 21 after BLM and stained with hematoxylin and eosin or Masson's trichrome (*see* online supplement for details).

### Transfection, Gene Expression, and Cellular Assays

Lung fibroblasts were stably transfected with either shRNA targeting CD148 (Sigma-Aldrich) or expression plasmid containing CD148 cDNA (Applied Biological Materials) by standard methods. Transient transfection assays were performed using FuGENE 6 transfection reagent (Promega) (26). Immunoblot and quantitative PCR (qPCR) analyses (27) and gel contraction assays (18) were performed as described. Cell viability was determined using 3-[4,5-dimethylthiazol-2-yl]-2,5-diphenyl tetrazolium bromide and trypan blue exclusion assays as described (26). Caspase-3 activity was measured using a kit (#K006–100; Biovision) (*see* online supplement for details).

### Statistical Analysis

Data are expressed as mean ± SEM. Kaplan-Meier survival curves were analyzed by log-rank tests to assess for differences in survival. For comparisons between two groups, we used Student's unpaired *t* test or Mann-Whitney nonparametric test. Statistical significance was defined as $P < 0.05$. One-way ANOVA, followed by Newman-Keuls or Tukey's *post hoc* test analysis or Kruskal-Wallis nonparametric test, was used for analysis of more than two groups.

## Results

### CD148 Is Downregulated in IPF

We measured the expression of CD148 in IPF or control lungs and in cell isolates from these lungs. CD148 protein and corresponding *Ptprj* mRNA concentrations were downregulated in IPF lungs compared with control lungs (Figures 1A and 1B). In IPF lung homogenates enriched for fibroblasts (Figure E1) (28), *Ptprj* mRNA was downregulated relative to fibroblast-enriched control lung homogenates (Figure 1C). Immunofluorescence staining revealed that CD148 costained with vimentin-positive cells in control lungs, indicating its expression in fibroblasts, whereas CD148 staining was significantly reduced in IPF lungs (Figure 1D). Costaining of IPF lungs with α-SMA and CD148 confirmed that CD148 is downregulated in myofibroblasts (Figure E2A). Analysis of a previously reported single-cell RNA sequencing dataset for IPF lung (29) revealed downregulated CD148 gene expression in IPF myofibroblasts compared with control lungs that did not achieve statistical significance (Figure E3). CD148 gene expression was modestly increased in IPF fibroblasts compared with control fibroblasts (Figure E3). Finally, we determined that CD148 was also expressed in alveolar epithelial type I and type II cells from control lungs (Figure E2B), with reduced staining (Figure E2B) and lower mRNA expression (Figure E4A) in AT2 cells from IPF lungs.

### CD148 Regulates the Profibrotic Phenotype of Lung Fibroblasts Derived from Patients with IPF

Fibroblasts isolated from IPF lungs have increased ECM production and resistance to cell death and apoptosis (30–32). To determine the role of CD148 in fibroblasts isolated from IPF lungs, we silenced CD148 expression in these cells using shCD148 (Figure 1E). CD148 silencing resulted in higher gene expression of *Fn* (fibronectin) and *Col1a1* (collagen 1a1) in IPF-derived lung fibroblasts relative to scramble (Scr)-transfected IPF fibroblasts (Figure 1F). Furthermore, IPF fibroblasts were resistant to cell death induced by Fas ligand (FasL) (Figure E4B). This effect was enhanced in CD148-deficient cells (Figure 1G). Overexpression of CD148 using stable lentiviral transduction with pLenti-CD148-HA (Figure 1H) resulted in downregulation of ECM gene expression (*Fn* and *Col1a1*) (Figure 1I), increased cell death (Figure 1J), and enhanced caspase-3 activity (Figure E4C).

### CD148 Deficiency in Fibroblasts Leads to Increased Pulmonary Fibrosis in BLM-challenged Mice

To investigate the role of CD148 in pulmonary fibrosis, we generated mice with a fibroblast-specific conditional deletion of CD148 ($Ptprj^{fl/fl}$ $Col1a2^{Cre-ER(T)+/0}$). CD148 was deleted in lung fibroblasts isolated from tamoxifen-treated $Ptprj^{fl/fl}$ $Col1a2^{Cre-ER(T)+/0}$ mice (Figure E5A). We exposed $Ptprj^{fl/fl}$ $Col1a2^{Cre-ER(T)+/0}$ mice or $Col1a2^{Cre-ER(T)+/0}$ (control) mice to BLM to induce pulmonary fibrosis. At 21 days after BLM instillation, $Ptprj^{fl/fl}$ $Col1a2^{Cre-ER(T)+/0}$ mice displayed greater lung interstitial thickening compared with control mice (Figure E5B). The fibroblast-specific CD148-deficient mice also displayed markedly higher lung collagen content by Masson's trichrome stain (Figure 2A) and hydroxyproline measurements (111.8 ± 18.5 μg/ml/lobe vs. 80.8 ± 8.8 μg/ml/lobe) (Figure 2B), reduced survival (Figure 2C), higher lung expression of α-SMA (Figures 2D and 2E) and profibrotic genes (*Fn*, *Col1a1*, and *Ctgf* [connective tissue growth factor]) (Figures 2F and 2G), and reduced CD148 expression (Figures 2D and 2E). There was no difference in inflammatory cell counts in the BAL fluid between the strains after BLM challenge (Figure E5C).

### CD148 Deficiency Leads to Increased Myofibroblast Differentiation, ECM Production, and Resistance to Apoptosis in Fibroblasts after TGF-β1 Stimulation

Lung fibroblasts from $Ptprj^{fl/fl}$ $Col1a2^{Cre-ER(T)+/0}$ and $Col1a2^{Cre-ER(T)+/0}$ (control) mice were isolated. CD148 deficiency enhanced TGF-β1–induced myofibroblast differentiation, as determined by α-SMA expression (Figure 2H) and increased the ECM gene expression (*Col1a1* and *Fn*) (Figure 2I). Cell contractility was higher in $Ptprj^{-/-}$ fibroblasts compared with wild-type cells after TGF-β1 treatment (Figure 2J). TGF-β1 stimulation induced resistance to FasL-induced cell death and apoptosis in wild-type cells, which was exacerbated in $Ptprj^{-/-}$ fibroblasts (Figure 2K). CD148 deficiency also increased cell proliferation induced by TGF-β1 in fibroblasts (Figure E5D).

### CD148 Deficiency Upregulates TGF-β1–induced PI3K/Akt/mTOR Signaling

CD148 regulates PI3K signaling by dephosphorylating (inactivating) the regulatory subunit of PI3K (p85) (11). As PI3K/Akt signaling is upregulated in activated fibroblasts and contributes to the development of pulmonary fibrosis (13, 15, 33), we investigated whether CD148 deficiency can enhance PI3K/Akt/mTOR signaling induced by TGF-β1 in lung fibroblasts derived from $Ptprj^{fl/fl}$ $Col1a2^{Cre-ER(T)+/0}$ mice. TGF-β1 treatment upregulated the phosphorylation of PI3K (p85 subunit), Akt, mTOR, and mTOR-related signaling proteins (p70 S6-kinase and S6) (Figure 3A). CD148 deficiency further increased the expression of phospho (p)-PI3K, p-Akt, p-mTOR, and downstream targets p-p70 and p-S6 (Figures 3A and E6A).

### CD148 Deficiency Inhibits Autophagy and Leads to p62 Accumulation in Lung Fibroblasts

Activation of mTOR suppresses autophagy in IPF-derived fibroblasts (30). As the absence of CD148 leads to activation of mTOR, a regulator of autophagy, we hypothesized that CD148 deficiency could potentially modulate autophagy. TGF-β1 downregulated

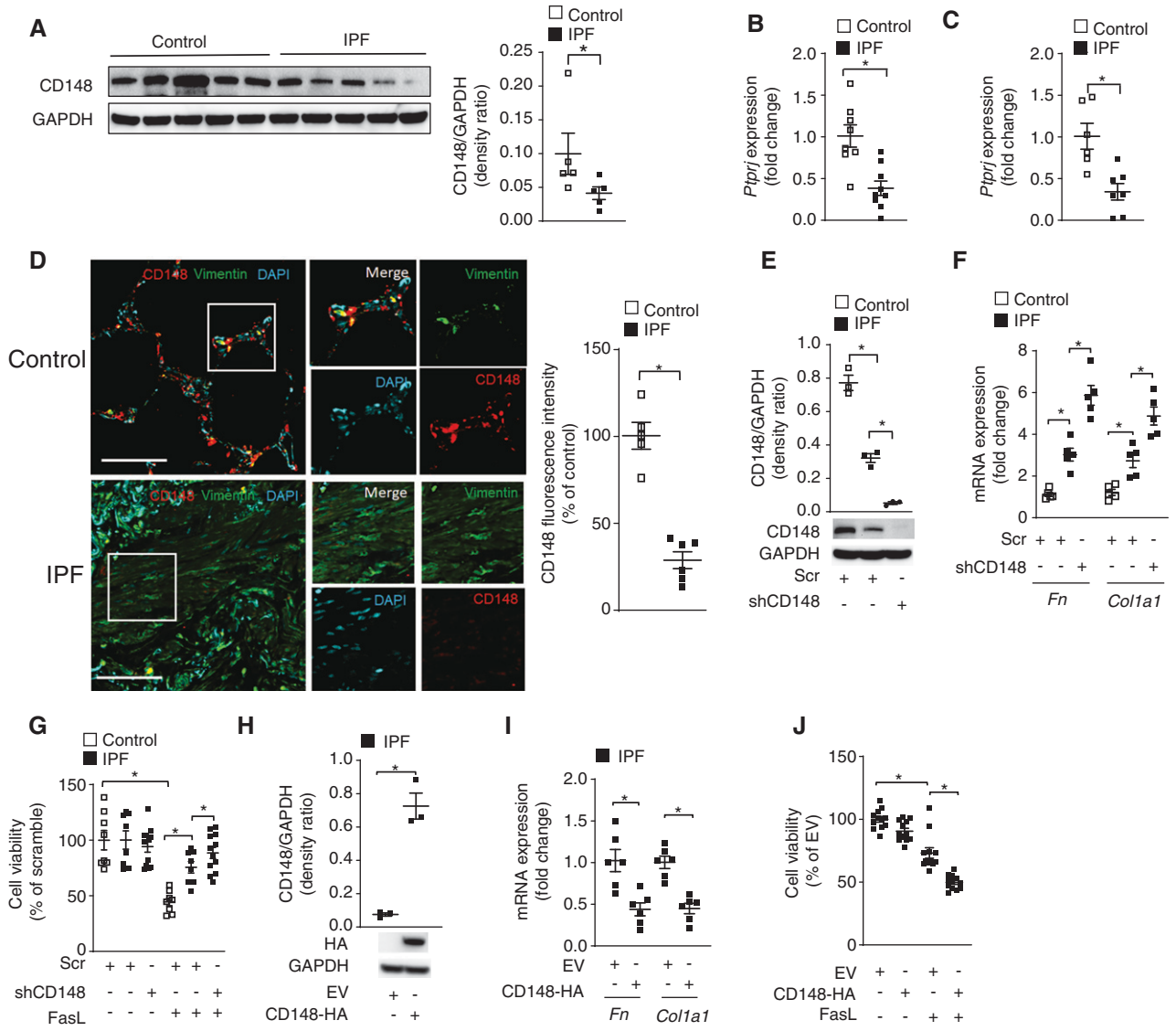


**Figure 1.** CD148 is downregulated in idiopathic pulmonary fibrosis (IPF) lung and contributes to profibrotic phenotype of IPF-derived lung fibroblasts. (*A*) CD148 protein expression levels were determined in lung homogenates from control patients ($n = 5$) and patients with IPF ($n = 5$). Densitometry (by ImageJ software). (*B*) Lung specimens from control patients ($n = 9$) and patients with IPF ($n = 10$) were homogenized and subjected to total RNA isolation. *Ptprj*/CD148 (receptor-like protein tyrosine phosphatase η) mRNA concentrations were assessed using quantitative PCR (qPCR). (*C*) Single-cell suspensions of control ($n = 6$) and IPF ($n = 7$) cells were enriched for fibroblasts (*see* Figure E1). mRNA expression of CD148 in fibroblast-enriched cell populations was assessed using qPCR. (*D*) Representative fluorescence microscopy images of CD148 (Cy3, red), Vimentin (GFP, green), and DAPI (blue) in control ($n = 4$) and IPF lung tissue ($n = 5$). Scale bars, 100 μm. Enlarged areas (clockwise from top right panel) represent Vimentin, CD148, DAPI, and merged image. CD148 fluorescence intensity was quantified by ImageJ. (*E* and *F*) Lung fibroblasts from nondisease (control) and IPF samples were transfected with scramble (Scr) or shCD148. (*E*) CD148 protein concentrations were measured by Western blot ($n = 3$). (*F*) mRNA concentrations of *Fn* (fibronectin) and *Col1a1* (collagen 1a1) were measured using qPCR ($n = 5$). (*G*) Scr and shCD148 transfected cells were seeded in 24-well plates and then treated with Fas ligand (FasL; 200 ng/ml) for 24 hours. After treatment, cell viability was determined using the 3-[4,5-dimethylthiazol-2-yl]-2,5-diphenyl tetrazolium bromide (MTT) assay ($n = 5$). (*H*) IPF-derived lung fibroblasts were stably transfected with empty vector (EV; pLenti-GIII-HA) or pLenti-GIII-CD148-HA (CD148-HA). The cells were lysed and subjected to Western blot to measure hemagglutinin tag (HA) ($n = 3$). (*I*) In EV- and CD148-HA–transfected cells, the expression of *Fn* and *Col1a1* were measured using qPCR ($n = 5$). (*J*) EV- and CD148-HA–transfected cells were seeded at equal amounts in 24-well plates and treated with FasL (200 ng/ml) for 24 hours. Cell viability was determined using the MTT assay ($n = 5$). Data are mean ± SEM. $^*P < 0.05$ by Mann-Whitney's unpaired nonparametric test (*E* and *H*), Student's unpaired *t* test (*B* and *C*), or one-way ANOVA (*F*–*J*).

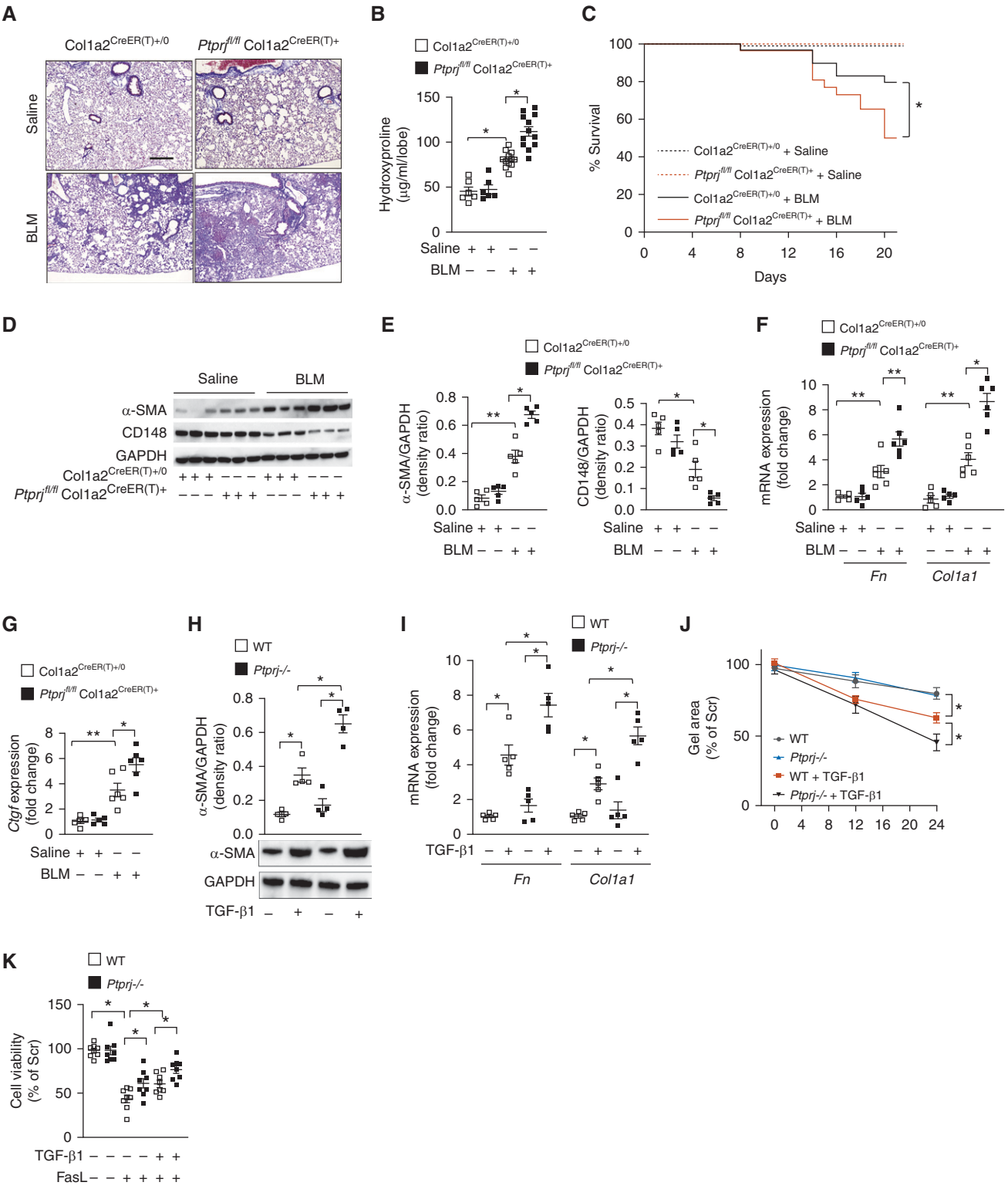


**Figure 2.** CD148 deficiency in fibroblasts worsens pulmonary fibrosis in bleomycin (BLM)-treated mice and increases fibroblast activation in response to TGF-β1. CD148 fibroblast-specific knockout mice (*Ptprj*$^{fl/fl}$ Col1a2$^{Cre-ER(T)+/0}$) were developed as described in METHODS. (*A*) *Ptprj*$^{fl/fl}$ Col1a2$^{Cre-ER(T)+/0}$ mice or Col1a2$^{Cre-ER(T)+/0}$ (wild-type [WT]) mice were exposed to BLM to induce lung fibrosis. At Day 21, mouse lungs were harvested and stained with Masson's trichrome ($n = 3$ for saline and $n = 5$ for BLM groups). (*B*) Hydroxyproline content was measured in the left lung of *Ptprj*$^{fl/fl}$ Col1a2$^{Cre-ER(T)+/0}$ mice ($n = 12$) and Col1a2$^{Cre-ER(T)+/0}$ (WT) mice ($n = 12$) exposed to BLM and *Ptprj*$^{fl/fl}$ Col1a2$^{Cre-ER(T)+/0}$ ($n = 6$) and Col1a2$^{Cre-ER(T)+/0}$ ($n = 6$) exposed to saline at Day 21. (*C*) Relative survival at Days 0–21 after BLM. (*D* and *E*) α-SMA and CD148 expression in

autophagy in lung fibroblasts, as reflected by reduced expression of microtubule-associated protein-1 LC3-II (active form) relative to LC3-I, and increased p62 expression (Figures 3B and E6B–E6D). CD148 deficiency exacerbated the suppression of autophagy by TGF-β1 (Figure 3B). We also examined relative autophagic flux using an LC3 turnover assay. Wild-type and *Ptprj*$^{-/-}$ fibroblasts were treated with chloroquine, which inhibits autophagosome-lysosome fusion and consumption of LC3B; this causes an accumulation of LC3-II that reflects the rate of autophagosome formation in the presence or absence of TGF-β1. CD148-deficient fibroblasts exhibited delayed LC3-II accumulation compared with control fibroblasts (Figures 3C and E6E). Decreased autophagosome formation was also observed in LC3-GFP transgenic lung fibroblasts in the absence of CD148 (Figures 3D and 3E). We next investigated whether the PI3K/mTOR axis and p62 upregulation are essential for the profibrotic response in CD148-deficient cells. We found that the increase of α-SMA in CD148-deficient cells in response to TGF-β1 was attenuated by wortmannin (a PI3K inhibitor), rapamycin (an mTOR inhibitor), and by p62 knockdown using sh-p62 (Figure E7).

### p62-Dependent NF-κB Activation Drives Transcriptional Regulation of Profibrotic Gene Expression

In cancer cells, p62 accumulation activates NF-κB by phosphorylating the IKK (inhibitor of κ-B kinase), resulting in degradation of the I-κB (κ-B inhibitor) and NF-κB nuclear translocation (34, 35). We thus sought to determine the relevance of this pathway in fibrogenesis. CD148-deficient cells (*Ptprj*$^{-/-}$) had higher concentrations of p-IKKα/β and p-I-κB (Figure 4A) and higher nuclear accumulation of NF-κB (p65 subunit) (Figure 4B) in response to TGF-β1. In CD148-deficient lung fibroblasts, *Col1a1* and *Acta2* mRNA expression levels were dependent on PI3K/Akt, mTOR, and p62 concentrations in response to TGF-β1 (Figures 4C and 4D). Interestingly, NF-κB activity in CD148-deficient cells was also dependent on PI3K/Akt, mTOR, and increased p62 concentrations (Figure 4E). The NF-κB inhibitor Bay 11–7082 inhibited TGF-β1–dependent increase in *Col1a1* expression in CD148-deficient cells (Figure 4F). Taken together, we demonstrate for the first time that decreased autophagy may transcriptionally modulate profibrotic gene expression by enhancing a p62/NF-κB signaling axis. Furthermore, we demonstrate that CD148 counteracts this signaling axis by inhibiting the PI3K/Akt/mTOR pathway. We also further confirmed the role of CD148 in regulating this pathway by overexpressing CD148 in human lung fibroblasts. As shown in Figure E8, overexpression of CD148 attenuated p62, p-IKKα/β, and p-I-κB expression and inhibited NF-κB luciferase activity in response to TGF-β1.

### SDC2-pep Inhibits Pulmonary Fibrosis via CD148 *In Vivo* and *In Vitro*

Two known extracellular proteins, thrombospondin and SDC2, can bind to CD148 and activate PTP activity (20, 36). Furthermore, we have previously identified an 18-aa sequence of the SDC2 ectodomain responsible for binding and activation of CD148 in endothelial cells (19, 20). We therefore evaluated the therapeutic potential of SDC2-pep in the mouse model of BLM-induced fibrosis. We exposed *Ptprj*$^{fl/fl}$ Col1a2$^{Cre-ER(T)+/0}$ mice or Col1a2$^{Cre-ER(T)+/0}$ (control) mice to BLM followed by the administration of SDC2-pep beginning on Day 10 after BLM, once daily, for 5 consecutive days. The SDC2-pep significantly inhibited pulmonary fibrosis in control mice, whereas in *Ptprj*$^{fl/fl}$ Col1a2$^{Cre-ER(T)+/0}$ mice the antifibrotic effect was significantly reduced but not absent (Figures 5A–5C and E9A), suggesting CD148-independent effects in lung fibroblasts or other cells in the fibrotic niche. SDC2-pep inhibited profibrotic gene expression (*Fn*, *Col1a1*, and *Ctgf)* in control mice (Figures 5C and 5D). There was a trend toward decreased BAL total cell counts in control mice treated with SDC2-pep but not in *Ptprj*$^{fl/fl}$ Col1a2$^{Cre-ER(T)+/0}$ mice (Figure E9B) after BLM.

Next, fibroblasts were stimulated with TGF-β1 in the absence or presence of SDC2-pep. TGF-β1 treatment increased the expression of p-Akt, p-mTOR, p62, p-IKKα/β, and α-SMA in wild-type fibroblasts (Figures 5E and E10). This effect was markedly abrogated by treatment with SDC2-pep. In contrast, the inhibitory effect of SDC2-pep on TGF-β1–dependent expression of these signaling proteins in *Ptprj*$^{-/-}$ fibroblasts was reduced (Figures 5E and E10). Similarly, SDC2-pep inhibited TGF-β1-induced *Fn* and *Col1a1* gene expression (Figure 5F) and cell contractility (Figure 5G) in wild-type fibroblasts. SDC-2 partially inhibited these effects in *Ptprj*$^{-/-}$ fibroblasts, which had markedly enhanced profibrotic responses to TGF-β1 stimulation (Figures 2G–2I). As shown in Figure E11, SDC2-pep dose-dependently inhibited *Col1a1* gene expression in wild-type fibroblasts and *Ptprj*$^{-/-}$ fibroblasts, further highlighting potential off-target effects of SDC2-pep in lung fibroblasts.

### SDC2-Pep Inhibits Pulmonary Fibrosis in Human IPF Fibroblasts and *Ex Vivo* PCLS

We next evaluated the therapeutic potential of SDC2-pep in human IPF fibroblasts. Treatment with SDC2-pep significantly inhibited the activation of the PI3K/Akt/mTOR pathway in human IPF fibroblasts (Figures 6A and E12). SDC2-pep significantly inhibited the expression of p-Akt and p-mTOR in human IPF fibroblasts in Scr-transfected, but not in shCD148-transfected, cells (Figure E10). SDC2-pep restored autophagy in human IPF fibroblasts in a CD148-dependent manner, as evidenced by increased relative LC3B-II expression and reduced p62 expression (Figure E12). SDC2-pep also inhibited ECM gene expression (*Fn* and *Col1a1*) (Figure 6A) and cell contractility

**Figure 2.** (*Continued*). harvested lungs were measured by Western blot ($n = 3$–5 for each condition). (*F* and *G*) Gene expression of *Fn* (fibronectin) and *Col1a1* (collagen 1a1) and *Ctgf* (connective tissue growth factor) in harvested lungs was measured using quantitative PCR (qPCR) ($n = 5$ for each condition). (*H* and *I*) Mouse lung fibroblasts from *Ptprj*$^{fl/fl}$ Col1a2$^{Cre-ER(T)+/0}$ mice (*Ptprj*$^{-/-}$) and Col1a2$^{Cre-ER(T)+/0}$ (WT) mice were isolated and treated with 4-hydroxytamoxifen (4-OHT; 1 μM) for 24 hours. After 4-OHT treatment, cells were exposed to TGF-β1 (10 ng/ml) for an additional 24 hours. After stimulation, cells were harvested. (*H*) Western blot ($n = 4$ for each condition). (*I*) mRNA concentrations of *Col1a1* and *Fn* were measured by qPCR ($n = 5$ for each condition). (*J*) Cells were mixed with collagen 1. Gel contractility was measured at 0, 12, and 24 hours after TGF-β1 (10 ng/ml) stimulation ($n = 6$ for each condition). (*K*) Cell death was induced by FasL (200 ng/ml). At 24 hours, cell viability was measured with 3-[4,5-dimethylthiazol-2-yl]-2,5-diphenyl tetrazolium bromide assay ($n = 5$ for each condition). Data are mean ± SEM. $^*P < 0.05$ and $^{**}P < 0.01$ by one-way ANOVA. FasL = Fas ligand.

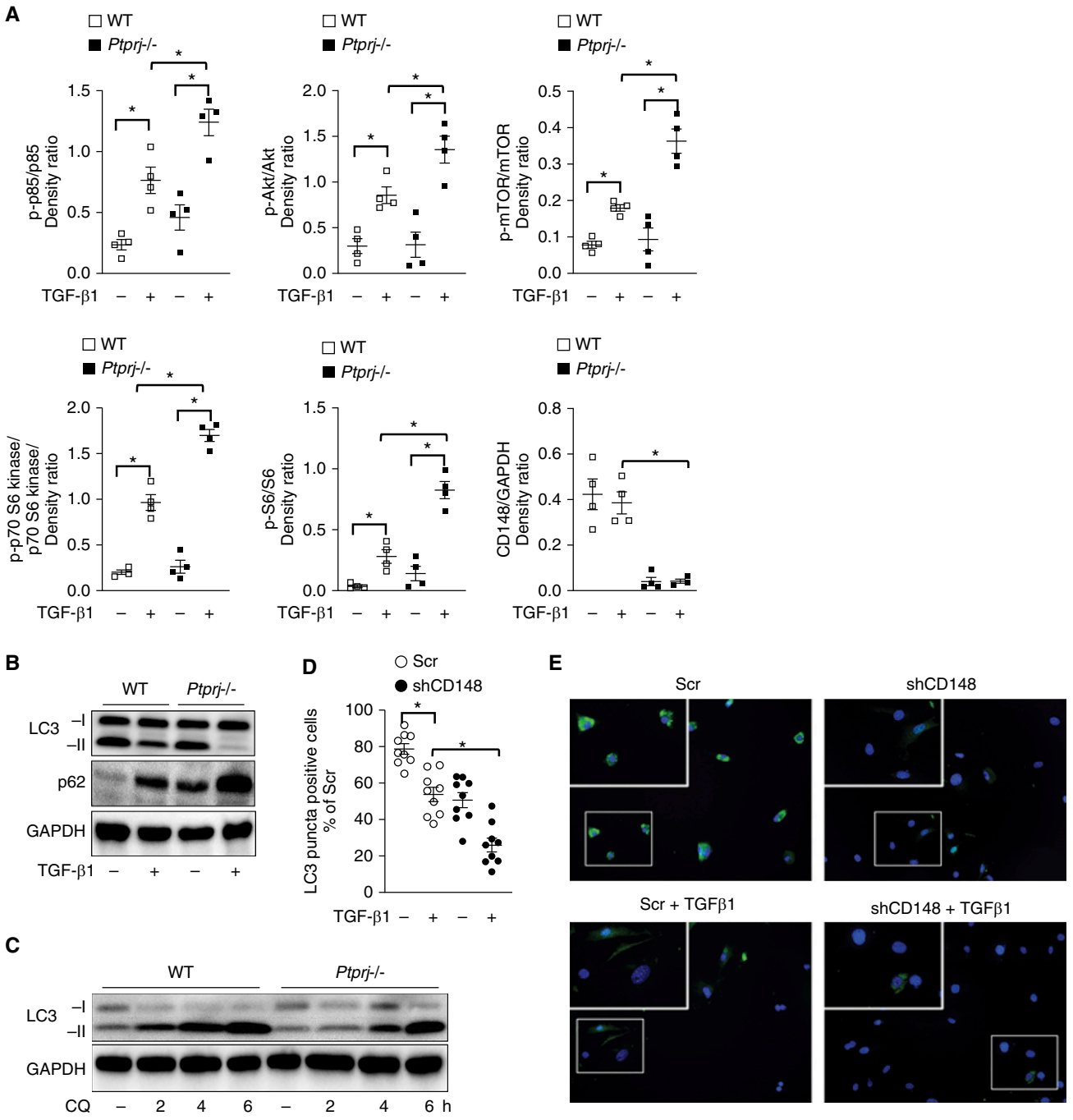


**Figure 3.** CD148 deficiency enhances PI3K/Akt/mTOR signaling, which results in low autophagy and high p62 expression in lung fibroblasts. (*A*) Mouse lung fibroblasts were isolated from *Ptprj*$^{fl/fl}$ Col1a2$^{Cre-ER(T)+/0}$ mice (*Ptprj*$^{-/-}$) and Col1a2$^{Cre-ER(T)+/0}$ mice (wild-type [WT]) and then treated with 4-hydroxytamoxifen (4-OHT; 1 μM) for 24 hours. After 4-OHT treatment, cells were exposed to TGF-β1 (10 ng/ml) for 24 hours. After stimulation, cells were harvested, and the expression of phospho (p)-p85 (Tyr458), p-Akt (Ser473), p-mTOR (Ser2448), p-p70 S6 kinase (Thr389), p-S6 ribosomal protein (Ser235/236), and CD148 ($n = 4$ for each condition) in lysates was determined by Western immunoblotting and corresponding densitometry (ImageJ software). Data were normalized to corresponding dephosphorylated forms or GAPDH. (*B*) WT and *Ptprj*$^{-/-}$ cells were stimulated with TGF-β1 (10 ng/ml) for 24 hours. Then cells were lysed, and LC3 (light chain-3B)-I, LC3-II, and p62 were measured by Western blot ($n = 4$). (*C*) WT and *Ptprj*$^{-/-}$ cells were incubated in starvation media (Hank's buffered salt solution without calcium/magnesium, containing 1% regular medium) for 24 hours. Then, autophagy flux was measured by LC3-II accumulation in the absence or presence of lysosomal acidification inhibitor chloroquine (25 μM) at 2, 4, and 6 hours ($n = 4$). (*D* and *E*) Lung fibroblasts from LC3-GFP transgenic mice were transfected with Scr or shCD148 (lentivirus). Cells were starved for 24 hours in the presence or absence of TGF-β1 (10 ng/ml), and then cells were treated with chloroquine (25 μM) for 4 hours. After treatment, cells were fixed and digital images (three images per sample) were taken using fluorescent microscope. Representative images are shown in *E*. LC3 puncta positive cells were quantified using ImageJ (*D*). Data are mean ± SEM. *$P < 0.05$ by one-way ANOVA. CQ = chloroquine; Scr = scramble.

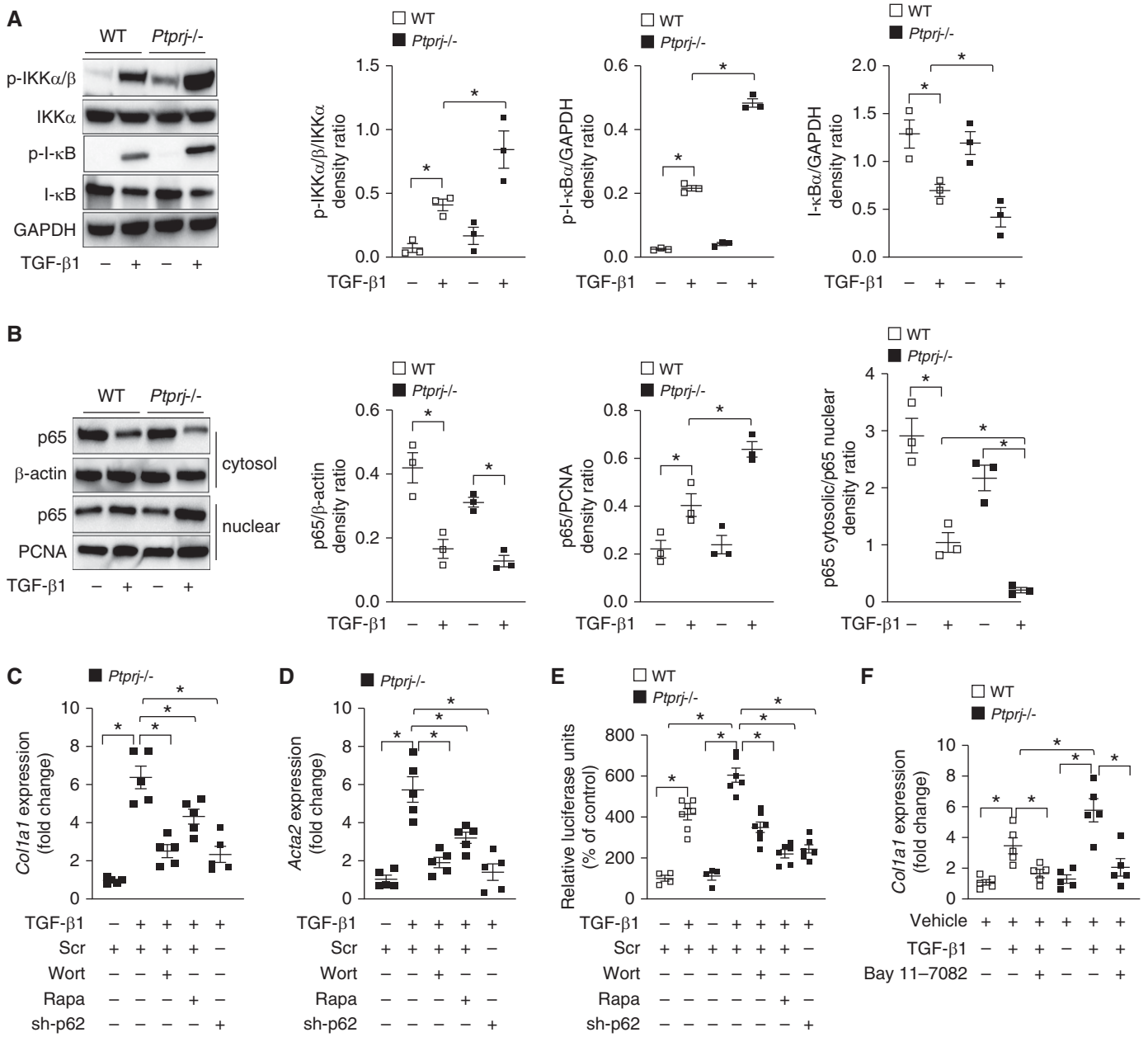


**Figure 4.** CD148 deficiency enhances PI3K/Akt/mTOR signaling, which results in enhanced NF-κB activation in lung fibroblasts. (*A*) Wild-type (WT) and *Ptprj*$^{-/-}$ cells were stimulated with TGF-β1 (10 ng/ml) for 24 hours. Cells were lysed and phospho (p)-IKKα/β, p-IκB, and IκB were measured by Western blot ($n = 4$). GAPDH was the standard. Bar graphs at right are the quantitation of corresponding proteins. (*B*) WT and *Ptprj*$^{-/-}$ cells were stimulated with TGF-β1 (10 ng/ml) for 24 hours. Cells were subjected to cytosol and nuclear protein fractionation. The p65 (NF-κB subunit) nuclear translocation was measured by Western blot ($n = 3$). β-actin and PCNA were used as cytosolic and nuclear markers, respectively. Bar graphs at right are the quantitation of corresponding proteins. The p65 cytosolic/nuclear ratio is shown (far right). Data are mean ± SEM. *$P < 0.05$ by Kruskal-Wallis nonparametric test (*C* and *D*) WT or *Ptprj*$^{-/-}$ cells were transfected with scramble (Scr) or shp62 (lentivirus). Cells were stimulated with TGF-β1 (10 ng/ml) in the presence or absence or wortmannin (wort; 50 nM) or rapamycin (rapa; 1 μM). At 24 hours, cells were harvested and subjected to quantitative PCR (qPCR) for *Col1a1* (collagen 1a1) or *Acta2* ($n = 5$). (*E*) WT or *Ptprj*$^{-/-}$ cells were transfected with NF-κB luciferase reporter plasmid in the presence or absence of Scr or shp62 or of wort (50 nM) or rapa (1 μM). Then, cells were treated with TGF-β1 (10 ng/ml) for 4 hours. Luciferase activity was measured as described in METHODS ($n = 4$ or 7). Data are mean ± SEM. *$P < 0.05$ by one-way ANOVA. (*F*) WT or *Ptprj*$^{-/-}$ cells were stimulated with TGF-β1 (10 ng/ml) in the presence or absence of the NF-κB inhibitor Bay 11–7082 (10 μM). mRNA concentrations of *Col1a1* were measured by qPCR ($n = 5$ for each condition). Data are mean ± SEM. *$P < 0.05$ by one-way ANOVA.

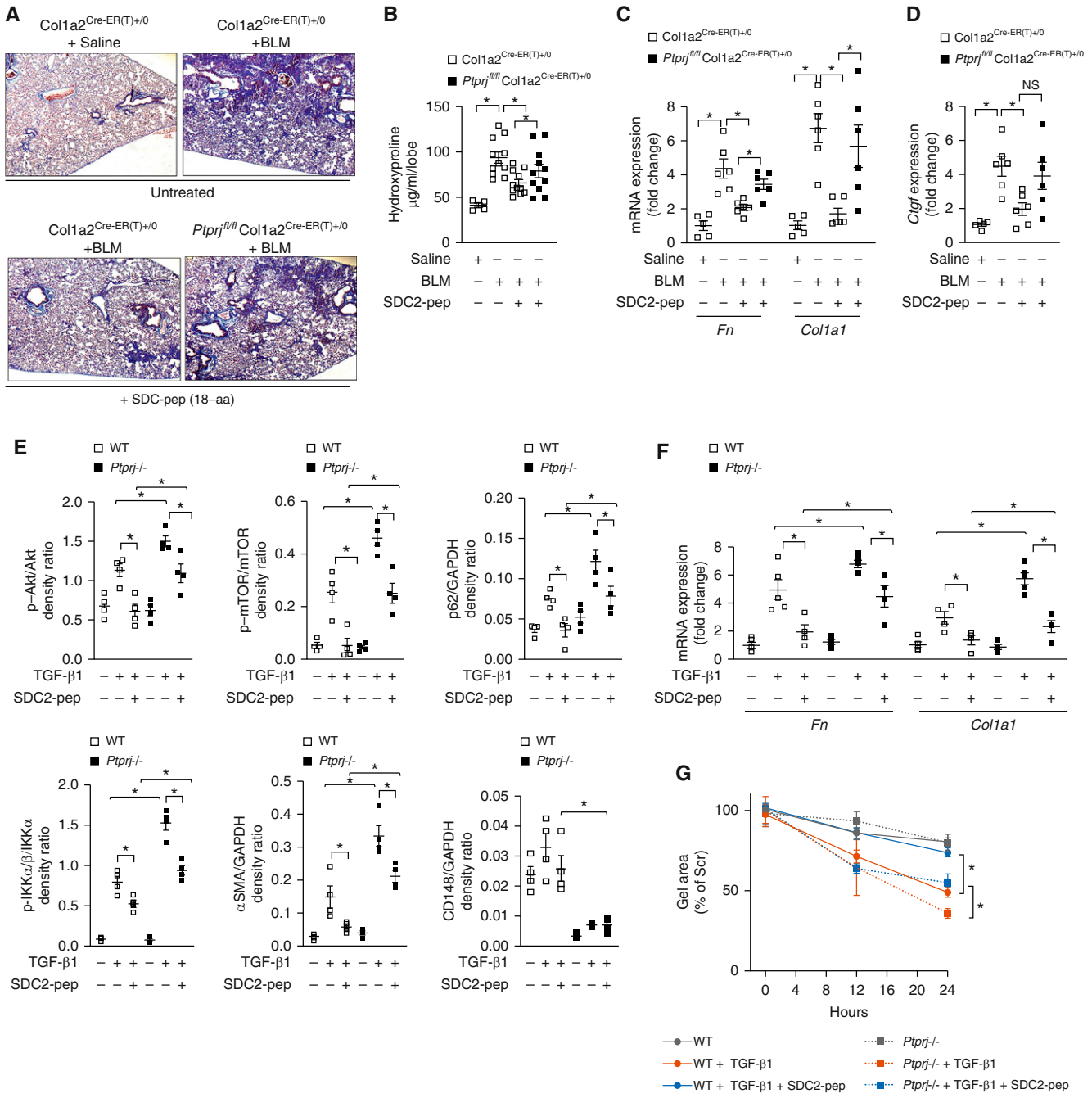


**Figure 5.** SDC2-ED 18-aa peptide (SDC2-pep) inhibits pulmonary fibrosis *in vivo*, upregulates autophagy by the downregulation of PI3K/Akt/mTOR signaling, and inhibits extracellular matrix gene expression in mouse fibroblasts via CD148. (*A–C*) *Ptprj*$^{fl/fl}$ Col1a2$^{Cre-ER(T)+/0}$ mice (fibroblast-specific CD148-deficient) and Col1a2$^{Cre-ER(T)+/0}$ (wild-type [WT]) mice were exposed to bleomycin (BLM). SDC2-pep (0.5 mg/kg) was intranasally delivered into WT and *Ptprj*$^{fl/fl}$ Col1a2$^{Cre-ER(T)+/0}$ mice 10 days after BLM injury. Treatments were repeated at Days 12, 14, 16, and 18. (*A*) At 24 days after BLM exposure, lungs were harvested and stained with Masson's trichrome ($n = 3$ for saline and $n = 5$ for BLM groups). (*B*) Hydroxyproline content was measured in the left lung of mice exposed to BLM ($n = 11$) or saline ($n = 5$). Gene expression of (*C*) *Fn* (fibronectin) and *Col1a1* (collagen 1a1) and (*D*) *Ctgf* (connective tissue growth factor) in harvested lungs were measured using quantitative PCR (qPCR) ($n = 5$ for each condition). (*E* and *F*) Mouse lung fibroblasts from *Ptprj*$^{fl/fl}$ Col1a2$^{Cre-ER(T)+/0}$ mice (*Ptprj*$^{-/-}$) and Col1a2$^{Cre-ER(T)+/0}$ mice (WT) were isolated and treated with 4-hydroxytamoxifen (4-OHT; 1 μM) for 24 hours. After 4-OHT treatment, cells were exposed to ±TGF-β1 (10 ng/ml) for an additional 24 hours in the absence or presence of SDC2-pep (5 μM). (*E*) Expression of phospho (p)-AKT/Akt, p-mTOR/mTOR, p62/GAPDH p-IKKα/β/IKKα, α-SMA/GAPDH, and CD148/GAPDH was determined by Western immunoblotting ($n = 4$) and corresponding densitometry (ImageJ software). Data are mean ± SEM. *$P < 0.05$ by one-way ANOVA. (*F*) mRNA concentrations of *Col1a1* and *Fn* were measured by qPCR ($n = 5$ for each condition). (*G*) After treatment, cells were mixed with collagen 1. Gel contractility was measured at 0, 12, and 24 hours after TGF-β1 stimulation ($n = 6$ for each condition). Data are mean ± SEM. *$P < 0.05$ by one-way ANOVA. NS = not significant.

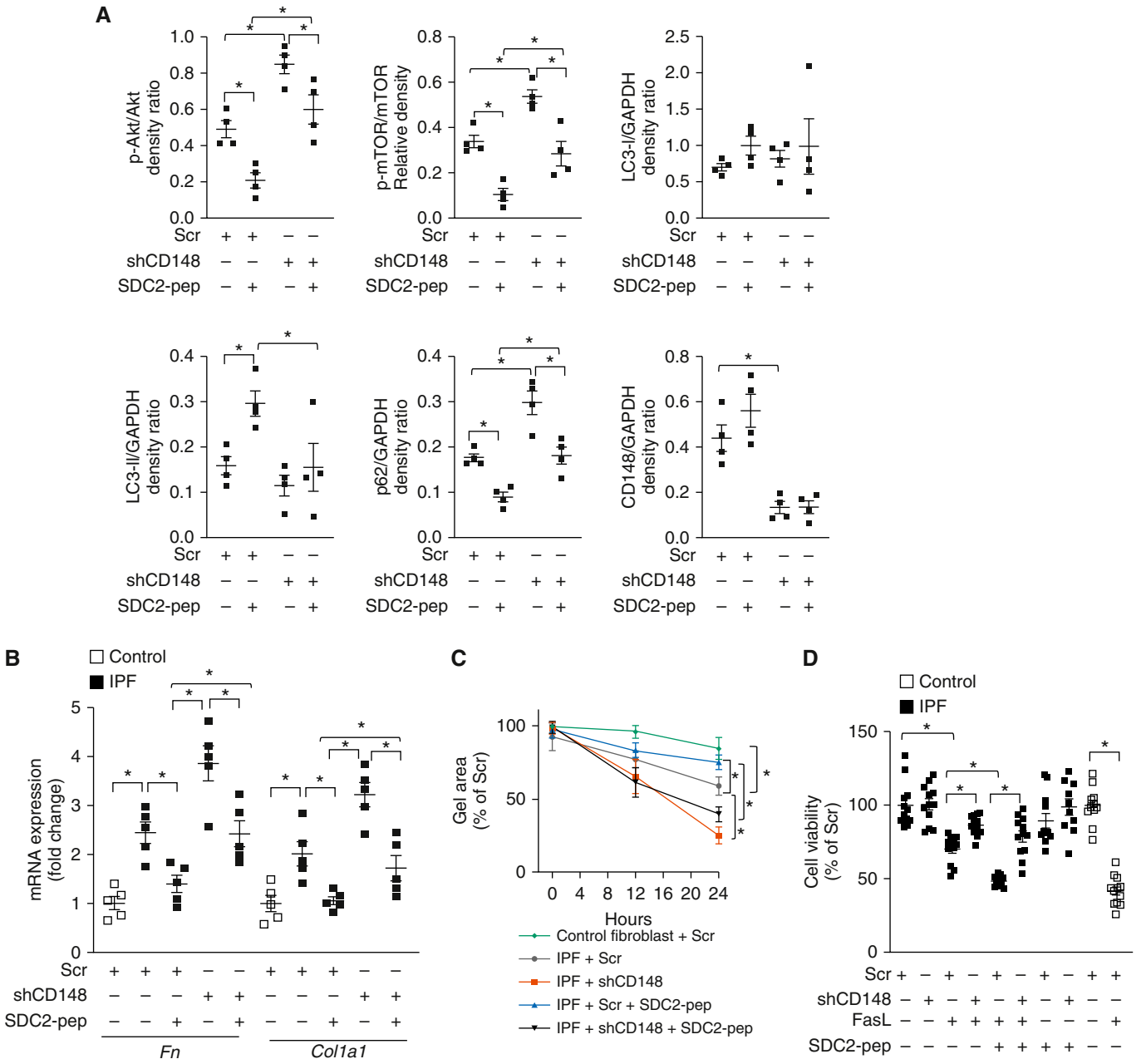


**Figure 6.** SDC2-ED 18-aa peptide (SDC2-pep) attenuates profibrotic gene expression in human idiopathic pulmonary fibrosis (IPF) fibroblasts. (*A*) IPF-derived lung fibroblasts were transfected with scramble (Scr) or shCD148. Then cells were treated with SDC2-pep (5 μM) for 24 hours. After incubation, phospho (p)-Akt (Ser473), p-mTOR (Ser2448), LC3 (light chain-3B), p62, and CD148 were measured by Western blot ($n = 4$). Band intensities were quantified using ImageJ software and were expressed as a ratio of band intensity relative to GAPDH. Data are mean ± SEM. *$P < 0.05$ by one-way ANOVA. (*B*) mRNA concentrations of *Fn* (fibronectin) and *Col1a1* (collagen 1a1) were measured by quantitative PCR ($n = 5$). (*C*) Scr- or shCD148-transfected control or IPF-derived lung fibroblasts were mixed with collagen 1. Gel contractility were measured at 0, 12, and 24 hours in the presence or absence of SDC2-pep (5 μM) ($n = 5$/group). (*D*) Scr- or shCD148-transfected control or IPF-derived lung fibroblasts were treated with FasL (200 ng/ml) for 24 hours in the presence or absence of SDC2-pep (5 μM) ($n = 7$). Cell viability was measured using 3-[4,5-dimethylthiazol-2-yl]-2,5-diphenyl tetrazolium bromide assay. Data are mean ± SEM. *$P < 0.05$ by one-way ANOVA. FasL = Fas ligand.

(Figure 6B), and these effects were reduced in the absence of CD148. Furthermore, SDC2-pep significantly enhanced FasL-induced cell death in IPF fibroblasts and, to a lesser extent, in CD148-deficient cells (Figure 6D).

Finally, we tested the potential antifibrotic effect of SDC2-pep in PCLS derived from IPF lung explants obtained at the time of transplant. We exposed PCLS from patients with IPF to SDC2-pep, which resulted in significantly decreased profibrotic gene expression (*Col1a1*, *Fn*, and *Acta2*) in Scr-transfected PCLS, and this effect was reduced in shCD148-transfected PCLS (Figures 7A and 7B). Flow cytometry in both fibroblasts

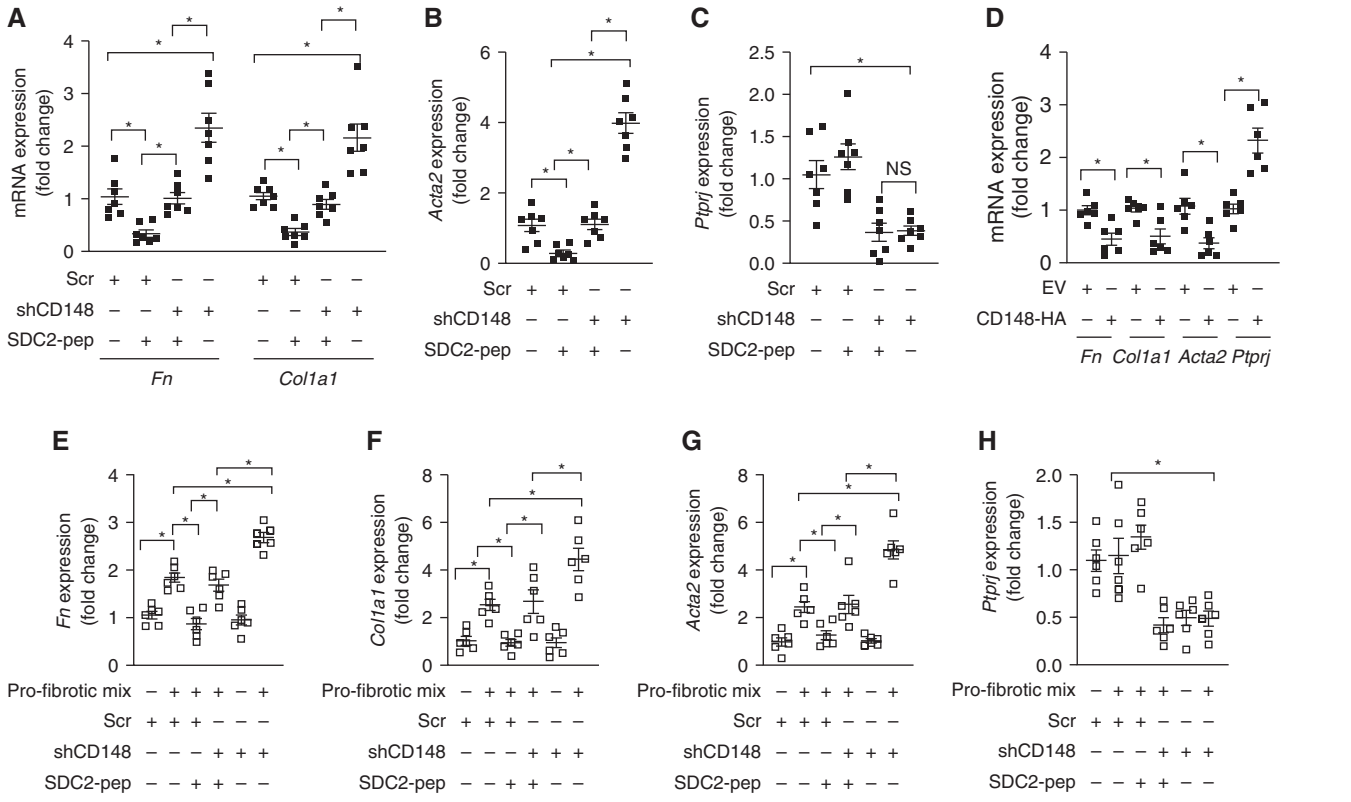


**Figure 7.** SDC2-ED 18-aa peptide (SDC2-pep) and CD148 overexpression attenuate profibrotic gene expression in precision-cut lung slices (PCLS) derived from idiopathic pulmonary fibrosis (IPF) lungs and from wild-type lungs subjected to profibrotic stimuli. (*A–D*) PCLS from IPF lungs were transfected with scramble (Scr), shCD148, or empty vector (EV) and CD148-HA. Then, PCLS were treated with SDC2-pep (5 μM) for 72 hours. After incubation, PCLS were digested for total RNA isolation. The expression of (*A*) *Fn* (fibronectin) and *Col1a1* (collagen 1a1), (*B*) *Acta2*, and (*C*) *Ptprj* (CD148) were measured by quantitative PCR (qPCR) ($n = 7$ for each condition). (*D*) mRNA concentrations of *Col1a1*, *Fn*, *Acta2*, and *Ptprj* (CD148) were measured by qPCR in EV- and CD148-overexpressing PCLS (CD148-HA). (*E–H*) PCLS from control lungs were transfected with Scr and shCD148 (lentivirus). Then, PCLSs were treated with profibrotic mix (FGF basic, 25 ng/ml; PDGF-BB, 10 ng/ml; and TGF-β1, 10 ng/ml) 72 hours with or without SDC2-pep (5 μM). After incubation, slices were digested for total RNA isolation. The expression of (*E*) *Fn*, (*F*) *Col1a1*, (*G*) *Acta2*, and (*H*) *Ptprj* were measured by qPCR. For *A–H*, $n = 6$ for each condition. Data are mean ± SEM. $^*P < 0.05$ by one-way ANOVA.

and epithelial cells isolated from PCLS indicated that shCD148 reduced gene expression by approximately 60% (Figures E13 and E14). SDC2-pep did not affect *Ptprj* gene expression in PCLS (Figure 7C), whereas shCD148 transfection of PCLS resulted in increased profibrotic responses (Figures 7A and 7B). Conversely, lentiviral overexpression of CD148 in PCLS from IPF lungs inhibited profibrotic gene expression (*Col1a1*, *Fn*, and *Acta2*) (Figure 7D). Finally, PCLS from control lungs were stimulated with a profibrotic mix in the presence or absence of SDC2-pep. SDC2-pep attenuated ECM gene expression (*Col1a1*, *Fn*, and *Acta2*) but not *Ptprj* expression in response to stimulation with a profibrotic mix in control PCLS. SDC-2-pep also partially inhibited ECM expression in CD148-deficient PCLS, which had markedly increased profibrotic responses to profibrotic mix (Figures 7E–7H). Taken together, our findings demonstrate that SDC2-pep inhibits lung fibrosis in human and experimental models of IPF predominantly through CD148, although CD148-independent effects may also contribute to its observed therapeutic effects. Our findings represent a new paradigm for the role of CD148 as a therapeutic target in IPF (Figure 8).

## Discussion

Here, we demonstrate that PTPRJ/CD148 regulates profibrotic responses and lung fibroblast activation in IPF. Importantly, we show that CD148 is downregulated in clinical samples of IPF lung, which in turn modulates profibrotic responses. In the current study, we use a conditional mouse approach to delineate the fibroblast-specific role of the receptor CD148 in mediating its antifibrotic effects in fibroblasts. We uncover a heretofore unknown role of NF-κB in fibrogenesis and ECM regulation and a novel downstream pathway of CD148 signaling. We also uncover a novel effector pathway by which PI3K/Akt-dependent modulation of autophagy via mTORC1 activation leads to aberrant p62 accumulation, which contributes to downstream NF-κB activation. In addition, we introduce a novel approach to therapeutic development in IPF, using a synthetic 18 amino-acid peptide derived from the SDC2 ectodomain. Because peptide-based approaches have been successfully developed for the treatment of diverse medical conditions (37), our current study demonstrates that a SDC2-based peptide mimetic is a potential innovative therapy for IPF.

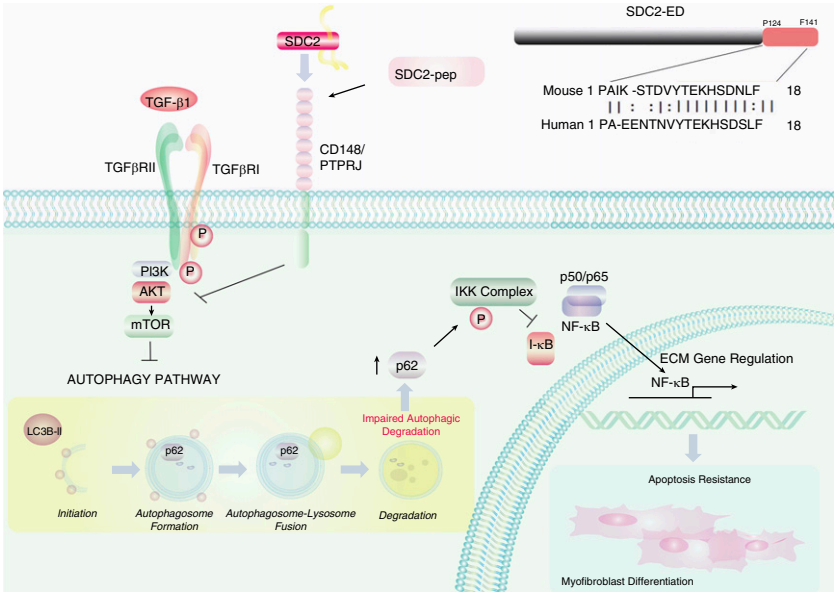


**Figure 8.** Schema depicting proposed antifibrotic effects of CD148 in fibroblasts. SDC2 (syndecan-2) via binding its receptor protein tyrosine phosphatase CD148/PTPRJ activates an antifibrotic pathway dependent on downregulation of TGF-β1–dependent signaling. TGF-β1 stimulates profibrotic effects via its receptor TGFβ-I/-II complex, which activates a PI3K/AKT/mTOR-dependent signaling pathway, culminating in the suppression of autophagy. The autophagy pathway, driven by LC3 (light chain-3B)-dependent formation of autophagosomes, directs the lysosomal degradation of autophagosome-sequestered cargo. Impaired autophagy is a characteristic feature of pulmonary fibrosis, which leads to aberrant accumulation of the autophagy substrate and cargo adaptor protein p62. Accumulated p62 promotes phosphorylation of the IKK (inhibitor of κ-B kinase) complex, leading to phosphorylation and dissociation of I-κB from the p65 subunit of NF-κB. The latter promotes p65/p50 assembly and migration of the NF-κB complex to the nucleus, where it stimulates profibrotic gene expression. NF-κB has also been implicated in apoptosis resistance and myofibroblast differentiation, characteristic of the profibrotic phenotype. Sequences (upper right) depict an 18-aa peptide region of the SDC2 ectodomain (SDC2-pep) with a high degree of homology between human and mouse sequences. SDC2-pep was tested in the current study as a therapeutic ligand of CD148/PTPRJ and found to have antifibrotic effects in idiopathic pulmonary fibrosis and models of pulmonary fibrosis. ECM = extracellular matrix.

CD148 was previously reported as a regulator of T-cell, B-cell, macrophage, and neutrophil function (38, 39). We demonstrate that CD148 downregulation in IPF fibroblasts contributes to cell activation, excessive ECM production, and resistance to apoptosis. In a mouse model of pulmonary fibrosis, targeted CD148 deficiency in fibroblasts exacerbates lung fibrosis by hyperactivation of PI3K/Akt/mTOR signaling, resulting in decreased autophagy. We have uncovered a novel mechanism by which impaired autophagy, via p62 accumulation, regulates NF-κB–dependent profibrotic responses in IPF lungs. Finally, we demonstrate that SDC2-pep, a CD148 agonist, can attenuate fibrosis in *in vitro*, *in vivo*, and *ex vivo* models of pulmonary fibrosis through CD148-dependent mechanisms by regulating PI3K/Akt/mTOR signaling, restoring autophagy, and downregulating ECM gene expression. Remarkably, the SDC2 mimetic peptide provides a robust antifibrotic effect in IPF fibroblasts despite a 50% reduction in CD148 expression in IPF lung tissue (Figures 1E–1G).

Although nintedanib, one of the two U.S. Food and Drug Administration–approved drugs to treat IPF, is a known PTK (protein tyrosine kinase) inhibitor, the role of endogenous PTK inhibitors (i.e., PTPs) in IPF remains incompletely understood. Prior studies investigating the regulation of cellular PTPs reveal divergent outcomes in experimental fibrosis with both potent profibrotic and antifibrotic effects reported (31, 40, 41). This may reflect the varying specificity of PTPs to dephosphorylate tyrosine residues and the differential subcellular localization and substrate specificities for signaling proteins (10). Furthermore, the majority of PTPs are expressed in different cell types, including immune cells, which may affect immune response or immune cell activation. Despite evidence implicating phosphatases in fibrogenesis, few investigative studies have developed effective therapies targeting phosphatase activity (42). We report here that SDC2-pep, which activates CD148, potently inhibits fibroblast activation and attenuates pulmonary fibrosis. The antifibrotic effect of SDC2-pep was largely attenuated, but not abolished, in fibroblast-specific CD148-deficient mice, suggesting that off-target effects in lung fibroblasts or regulation of additional receptor-mediated pathways in other cell types (e.g., alveolar epithelial cells) may mediate the therapeutic effects of SDC2-pep (17).

Autophagy is a cellular homeostatic process regulating the turnover of cellular organelles (i.e., mitochondria) and long-lived proteins. Although considered a prosurvival response, autophagy plays context-dependent roles in human disease progression (42). In IPF, low autophagy activity in fibroblasts may contribute to their profibrotic phenotype (43, 44). Here, we demonstrated that CD148 regulates autophagy via PI3K/Akt/mTOR signaling. However, CD148 deficiency also increases ECM gene expression via PI3K/Akt/mTOR signaling, suggesting transcriptional regulation of profibrotic gene expression. PI3K/Akt and mTOR activation may inhibit autophagy in activated fibroblasts. Thus, inhibition of the PI3K/Akt signaling pathway restores autophagy and inhibits fibrosis (30, 43). Although low autophagy is associated with a profibrotic phenotype, the underlying mechanisms remain unclear. Rangarajan and colleagues demonstrated that autophagy regulates ECM production by removing excessive cytosolic collagen via autophagosomal degradation. Thus, the activation of autophagy by AMPK (AMP-activated protein kinase) activators (i.e., metformin or AICAR [5-aminoimidazole-4-carboxamide riboside]) inhibited excessive collagen expression via autophagosomal degradation (45). Interestingly, AMPK activators also inhibited ECM gene expression, which is not directly attributed to autophagosomal degradation. Hence, we hypothesized that autophagy may regulate transcriptional responses through distinct mechanisms. We demonstrate that low autophagy results in upregulation of profibrotic gene expression by enabling p62 accumulation, which is inversely correlated with autophagy activity (46). p62/SQSTM1 (sequestosome 1, ZIP3) contains multiple

major domains, such as PB1 and ZZ, that confer the ability to interact with key components involved in essential signaling pathways. Importantly, p62 can regulate NF-κB via activation of IKK (46), which may contribute to cell survival, ECM production, and myofibroblast transformation (47).

Our studies have uncovered a distinct role for NF-κB in profibrotic responses, which is of broad significance because NF-κB transcriptional regulation is commonly associated with inflammatory, not fibroproliferative, responses. We found that CD148 deficiency resulted in NF-κB hyperactivation, which was required for enhanced ECM production in IPF fibroblasts. The hyperactivation of NF-κB by impaired autophagy provides a novel mechanistic link not previously characterized for IPF and experimental fibrosis. Consistently, the ECM protein *Fn* is tightly regulated by NF-κB, although there are no binding sites for NF-κB evident in the *Col1a1* and *Acta2* promoter regions (48, 49). Nevertheless, we found that CD148-deficient cells overexpress Col1a1 and α-SMA, and this effect was attenuated by an NF-κB inhibitor. NF-κB may possibly regulate ECM genes by indirect mechanisms, such that its subunits may interact with other transcription factors and regulate their transcriptional activity. For example, the p65 and p50 subunits of NF-κB can regulate the transcriptional activity of serum response factor and activator protein-1, which are implicated in *Acta2* and *Col1a1* gene expression, respectively (50, 51). NF-κB has also been shown to regulate the expression of multiple cytokines and chemokines now grouped as the senescence-associated secretory phenotype factors (e.g., IL-8, IL-6, and MCP-1) (52), which are associated with age-dependent organ fibrosis. Thus, further studies are needed to determine whether CD148 modulates cell senescence in fibrosis through the regulation of p62/NF-κB signaling.

Our findings highlight CD148 as a key regulator of profibrotic responses in pulmonary fibroblasts. However, our data also suggest that CD148 is also downregulated in alveolar epithelial type I and alveolar epithelial type II cells from IPF lungs compared with control lungs. Interestingly, CD148 may regulate epithelial tight junctions by dephosphorylating tight junction proteins such as ZO-1 and occludin (53). Given that lung epithelial cell injury, integrity, and hyperplasia represent hallmarks of lung fibrogenesis (1), future studies using conditional knockout approaches may elucidate new roles for CD148 in regulating lung epithelial cell responses to alveolar injury. Because immune cells may also contribute to fibrogenesis, the functional role of CD148 in immune cells also warrants investigation in fibrosis. Although we have identified a critical role of CD148 in fibroblast activation in pulmonary fibrosis and its underlying signaling processes, including novel roles for autophagy and NF-κB–dependent signaling, this work has several other limitations. First, the precise mechanisms and key intermolecular interactions by which NF-κB regulates profibrotic genes remain incompletely elucidated, and further investigation will be needed. Second, the therapeutic effects of SDC-pep are not limited to CD148-dependent effects in fibroblasts, as SDC2 may have targeted effects in other fibroblast receptor or cell types, including epithelial cells in the fibrotic niche, which may account for partial therapeutic effects observed in fibroblast-specific $Ptprj^{-/-}$ mice. Additional studies are required to elucidate specific secondary targets of the SDC2-pep. Finally, analysis of archival single-cell RNA sequencing data (29) did not fully recapitulate the downregulation of myofibroblast CD148 observed in the current study. However, the differences between myofibroblast and fibroblast CD148 expression are intriguing and may further support the notion that CD148 regulates fibroblast/myofibroblast phenotypes in health and disease. Further translational studies using lungs obtained from independent cohorts and at various stages of disease progression will be needed to confirm the antifibrotic effects of CD148 and the efficacy of its therapeutic ligands. In conclusion, our findings highlight CD148 as a novel and promising avenue for therapeutic targeting in IPF. ■

**Author disclosures** are available with the text of this article at www.atsjournals.org.

## References


1. Martinez FJ, Collard HR, Pardo A, Raghu G, Richeldi L, Selman M, *et al.* Idiopathic pulmonary fibrosis. *Nat Rev Dis Primers* 2017;3:17074.
2. Chambers RC, Mercer PF. Mechanisms of alveolar epithelial injury, repair, and fibrosis. *Ann Am Thorac Soc* 2015;12:S16–S20.
3. Richeldi L, du Bois RM, Raghu G, Azuma A, Brown KK, Costabel U, *et al.*; INPULSIS Trial Investigators. Efficacy and safety of nintedanib in idiopathic pulmonary fibrosis. *N Engl J Med* 2014;370:2071–2082.
4. Richeldi L, Costabel U, Selman M, Kim DS, Hansell DM, Nicholson AG, *et al.* Efficacy of a tyrosine kinase inhibitor in idiopathic pulmonary fibrosis. *N Engl J Med* 2011;365:1079–1087.
5. Harrod TR, Justement LB. Evaluating function of transmembrane protein tyrosine phosphatase CD148 in lymphocyte biology. *Immunol Res* 2002; 26:153–166.
6. Gayà A, Pirotto F, Palou E, Autschbach F, Del Pozo V, Solé J, *et al.* CD148, a new membrane tyrosine phosphatase involved in leukocyte function. *Leuk Lymphoma* 1999;35:237–243.
7. Fournier P, Dussault S, Fusco A, Rivard A, Royal I. Tyrosine phosphatase PTPRJ/DEP-1 is an essential promoter of vascular permeability, angiogenesis, and tumor progression. *Cancer Res* 2016;76:5080–5091.
8. Iuliano R, Trapasso F, Le Pera I, Schepis F, Samà I, Clodomiro A, *et al.* An adenovirus carrying the rat protein tyrosine phosphatase eta suppresses the growth of human thyroid carcinoma cell lines in vitro and in vivo. *Cancer Res* 2003;63:882–886.
9. Kellie S, Craggs G, Bird IN, Jones GE. The tyrosine phosphatase DEP-1 induces cytoskeletal rearrangements, aberrant cell-substratum interactions and a reduction in cell proliferation. *J Cell Sci* 2004;117: 609–618.
10. Julien SG, Dubé N, Hardy S, Tremblay ML. Inside the human cancer tyrosine phosphatome. *Nat Rev Cancer* 2011;11:35–49.
11. Tsuboi N, Utsunomiya T, Roberts RL, Ito H, Takahashi K, Noda M, *et al.* The tyrosine phosphatase CD148 interacts with the p85 regulatory subunit of phosphoinositide 3-kinase. *Biochem J* 2008;413:193–200.
12. Omerovic J, Clague MJ, Prior IA. Phosphatome profiling reveals PTPN2, PTPRJ and PTEN as potent negative regulators of PKB/Akt activation in Ras-mutated cancer cells. *Biochem J* 2010;426:65–72.
13. Kral JB, Kuttke M, Schrottmaier WC, Birnecker B, Warszawska J, Wernig C, *et al.* Sustained PI3K Activation exacerbates BLM-induced Lung Fibrosis via activation of pro-inflammatory and pro-fibrotic pathways. *Sci Rep* 2016;6:23034.
14. Wygrecka M, Zakrzewicz D, Taborski B, Didiasova M, Kwapiszewska G, Preissner KT, *et al.* TGF-β1 induces tissue factor expression in human lung fibroblasts in a PI3K/JNK/Akt-dependent and AP-1-dependent manner. *Am J Respir Cell Mol Biol* 2012;47:614–627.
15. White ES, Thannickal VJ, Carskadon SL, Dickie EG, Livant DL, Markwart S, *et al.* Integrin alpha4beta1 regulates migration across basement membranes by lung fibroblasts: a role for phosphatase and tensin homologue deleted on chromosome 10. *Am J Respir Crit Care Med* 2003;168:436–442.

16. Bartlett AH, Hayashida K, Park PW. Molecular and cellular mechanisms of syndecans in tissue injury and inflammation. *Mol Cells* 2007;24:153–166.
17. Shi Y, Gochuico BR, Yu G, Tang X, Osorio JC, Fernandez IE, *et al.* Syndecan-2 exerts antifibrotic effects by promoting caveolin-1-mediated transforming growth factor-$\beta$ receptor I internalization and inhibiting transforming growth factor-$\beta$1 signaling. *Am J Respir Crit Care Med* 2013;188:831–841.
18. Tsoyi K, Chu SG, Patino-Jaramillo NG, Wilder J, Villalba J, Doyle-Eisele M, *et al.* Syndecan-2 attenuates radiation-induced pulmonary fibrosis and inhibits fibroblast activation by regulating PI3K/Akt/ROCK pathway via CD148. *Am J Respir Cell Mol Biol* 2018;58:208–215.
19. De Rossi G, Evans AR, Kay E, Woodfin A, McKay TR, Nourshargh S, *et al.* Shed syndecan-2 inhibits angiogenesis. *J Cell Sci* 2014;127:4788–4799.
20. Whiteford JR, Xian X, Chaussade C, Vanhaesebroeck B, Nourshargh S, Couchman JR. Syndecan-2 is a novel ligand for the protein tyrosine phosphatase receptor CD148. *Mol Biol Cell* 2011;22:3609–3624.
21. Tsoyi K, Chu S, Xiong K, Ith B, Exposito A, Poli S, *et al.* Receptor type protein tyrosine phosphatase $\eta$ (PTPRJ/CD148) deficiency in fibroblasts leads to increased fibrosis by regulating PI3K/Akt/mTOR signaling, autophagy and p62 Level. *Am J Respir Crit Care Med* 2020;201:A1235.
22. Tsoyi K, Hall SR, Dalli J, Colas RA, Ghanta S, Ith B, *et al.* Carbon monoxide improves efficacy of mesenchymal stromal cells during sepsis by production of specialized proresolving lipid mediators. *Crit Care Med* 2016;44:e1236–e1245.
23. Adolph TE, Tomczak MF, Niederreiter L, Ko HJ, Böck J, Martinez-Naves E, *et al.* Paneth cells as a site of origin for intestinal inflammation. *Nature* 2013;503:272–276.
24. Uhl FE, Vierkotten S, Wagner DE, Burgstaller G, Costa R, Koch I, *et al.* Preclinical validation and imaging of Wnt-induced repair in human 3D lung tissue cultures. *Eur Respir J* 2015;46:1150–1166.
25. Bai Y, Krishnamoorthy N, Patel KR, Rosas I, Sanderson MJ, Ai X. Cryopreserved human precision-cut lung slices as a bioassay for live tissue banking: a viability study of bronchodilation with bitter-taste receptor agonists. *Am J Respir Cell Mol Biol* 2016;54:656–663.
26. Tsoyi K, Kim HJ, Shin JS, Kim DH, Cho HJ, Lee SS, *et al.* HO-1 and JAK-2/STAT-1 signals are involved in preferential inhibition of iNOS over COX-2 gene expression by newly synthesized tetrahydroisoquinoline alkaloid, CKD712, in cells activated with lipopolysacchride. *Cell Signal* 2008;20:1839–1847.
27. Schmittgen TD, Livak KJ. Analyzing real-time PCR data by the comparative C(T) method. *Nat Protoc* 2008;3:1101–1108.
28. Fujino N, Kubo H, Ota C, Suzuki T, Suzuki S, Yamada M, *et al.* A novel method for isolating individual cellular components from the adult human distal lung. *Am J Respir Cell Mol Biol* 2012;46:422–430.
29. Adams TS, Schupp JC, Poli S, Ayaub EA, Neumark N, Ahangari F, *et al.* Single-cell RNA-seq reveals ectopic and aberrant lung-resident cell populations in idiopathic pulmonary fibrosis. *Sci. Adv* 2020;6:eaba1983.
30. Romero Y, Bueno M, Ramirez R, Álvarez D, Sembrat JC, Goncharova EA, *et al.* mTORC1 activation decreases autophagy in aging and idiopathic pulmonary fibrosis and contributes to apoptosis resistance in IPF fibroblasts. *Aging Cell* 2016;15:1103–1112.
31. Bamberg A, Redente EF, Groshong SD, Tuder RM, Cool CD, Keith RC, *et al.* Protein tyrosine phosphatase-N13 promotes myofibroblast resistance to apoptosis in idiopathic pulmonary fibrosis. *Am J Respir Crit Care Med* 2018;198:914–927.
32. Nho RS, Peterson M, Hergert P, Henke CA. FoxO3a (Forkhead Box O3a) deficiency protects Idiopathic Pulmonary Fibrosis (IPF) fibroblasts from type I polymerized collagen matrix-induced apoptosis via caveolin-1 (cav-1) and Fas. *PLoS One* 2013;8:e61017.
33. Nho RS, Hergert P. IPF fibroblasts are desensitized to type I collagen matrix-induced cell death by suppressing low autophagy via aberrant Akt/mTOR kinases. *PLoS One* 2014;9:e94616.
34. Duran A, Linares JF, Galvez AS, Wikenheiser K, Flores JM, Diaz-Meco MT, *et al.* The signaling adaptor p62 is an important NF-kappaB mediator in tumorigenesis. *Cancer Cell* 2008;13:343–354.
35. Moscat J, Diaz-Meco MT. p62: a versatile multitasker takes on cancer. *Trends Biochem Sci* 2012;37:230–236.
36. Takahashi K, Mernaugh RL, Friedman DB, Weller R, Tsuboi N, Yamashita H, *et al.* Thrombospondin-1 acts as a ligand for CD148 tyrosine phosphatase. *Proc Natl Acad Sci USA* 2012;109:1985–1990.
37. Fosgerau K, Hoffmann T. Peptide therapeutics: current status and future directions. *Drug Discov Today* 2015;20:122–128.
38. Zhu JW, Doan K, Park J, Chau AH, Zhang H, Lowell CA, *et al.* Receptor-like tyrosine phosphatases CD45 and CD148 have distinct functions in chemoattractant-mediated neutrophil migration and response to S. aureus. *Immunity* 2011;35:757–769.
39. Skrzypczynska KM, Zhu JW, Weiss A. Positive regulation of lyn kinase by CD148 is required for B cell receptor signaling in B1 but not B2 B cells. *Immunity* 2016;45:1232–1244.
40. Aschner Y, Khalifah AP, Briones N, Yamashita C, Dolgonos L, Young SK, *et al.* Protein tyrosine phosphatase $\alpha$ mediates profibrotic signaling in lung fibroblasts through TGF-$\beta$ responsiveness. *Am J Pathol* 2014;184:1489–1502.
41. Tzouvelekis A, Yu G, Lino Cardenas CL, Herazo-Maya JD, Wang R, Woolard T, *et al.* SH2 domain-containing phosphatase-2 is a novel anti-fibrotic regulator in pulmonary fibrosis. *Am J Respir Crit Care Med* 2017;195:500–514.
42. Lazo JS, Sharlow ER. Drugging undruggable molecular cancer targets. *Annu Rev Pharmacol Toxicol* 2016;56:23–40.
43. Patel AS, Lin L, Geyer A, Haspel JA, An CH, Cao J, *et al.* Autophagy in idiopathic pulmonary fibrosis. *PLoS One* 2012;7:e41394.
44. Bueno M, Lai YC, Romero Y, Brands J, St Croix CM, Kamga C, *et al.* PINK1 deficiency impairs mitochondrial homeostasis and promotes lung fibrosis. *J Clin Invest* 2015;125:521–538.
45. Rangarajan S, Bone NB, Zmijewska AA, Jiang S, Park DW, Bernard K, *et al.* Metformin reverses established lung fibrosis in a bleomycin model. *Nat Med* 2018;24:1121–1127.
46. Puissant A, Fenouille N, Auberger P. When autophagy meets cancer through p62/SQSTM1. *Am J Cancer Res* 2012;2:397–413.
47. Mia MM, Bank RA. The I$\kappa$B kinase inhibitor ACHP strongly attenuates TGF$\beta$1-induced myofibroblast formation and collagen synthesis. *J Cell Mol Med* 2015;19:2780–2792.
48. Büttner C, Skupin A, Rieber EP. Transcriptional activation of the type I collagen genes COL1A1 and COL1A2 in fibroblasts by interleukin-4: analysis of the functional collagen promoter sequences. *J Cell Physiol* 2004;198:248–258.
49. Shimizu RT, Blank RS, Jervis R, Lawrenz-Smith SC, Owens GK. The smooth muscle alpha-actin gene promoter is differentially regulated in smooth muscle versus non-smooth muscle cells. *J Biol Chem* 1995;270:7631–7643.
50. Franzoso G, Carlson L, Brown K, Daucher MB, Bressler P, Siebenlist U. Activation of the serum response factor by p65/NF-kappaB. *EMBO J* 1996;15:3403–3412.
51. Fujioka S, Niu J, Schmidt C, Sclabas GM, Peng B, Uwagawa T, *et al.* NF-kappaB and AP-1 connection: mechanism of NF-kappaB-dependent regulation of AP-1 activity. *Mol Cell Biol* 2004;24:7806–7819.
52. Salminen A, Kauppinen A, Kaarniranta K. Emerging role of NF-$\kappa$B signaling in the induction of senescence-associated secretory phenotype (SASP). *Cell Signal* 2012;24:835–845.
53. Sallee JL, Burridge K. Density-enhanced phosphatase 1 regulates phosphorylation of tight junction proteins and enhances barrier function of epithelial cells. *J Biol Chem* 2009;284:14997–15006.